

Optimized Received Signal Strength-Based Radio Map Interpolation for Indoor Positioning Systems

Hui Wen Khoo

 <https://orcid.org/0000-0001-7551-2519>

Multimedia University, Malaysia

Yin Hoe Ng

Multimedia University, Malaysia

Chee Keong Tan

Monash University, Malaysia

ABSTRACT

The most viable strategy to establish a dependable indoor positioning system is by employing the received signal strength (RSS) based fingerprinting technique, which encompasses both the offline and online phases. The offline phase involves constructing a radio map, which can be arduous in vast indoor environments. To tackle this, radio map interpolation is often used to interpolate RSS by utilizing the RSS recorded at a coarser level of known reference points (RPs). This paper proposes a novel RSS-based radio map interpolation to enhance the existing inverse distance weighting (IDW) interpolation technique. The method divides the deployment area into zones and optimizes the density of known RPs in each zone based on the number of access points (APs) with average RSS exceeding the threshold. It allocates higher RP density for the zones with poor AP coverage and reduces it for well-covered zones. Results demonstrate that the proposed method achieves substantial improvements over the baseline IDW scheme in average positioning error of up to 6.58% at the floor level and 3.77% overall.

KEYWORDS

Indoor Positioning, BLE Fingerprint, Wi-Fi Fingerprint, Received Signal Strength (RSS), Radio Map Interpolation

INTRODUCTION

The proliferation of location-based services in today's world, which employ a user's geographic location to supply location-specific data, has led to a greater need for precise and up-to-date indoor positioning systems that can support indoor location-based services (Tan et al., 2021). Although the GPS is widely employed to enable outdoor wayfinding and positioning, the system is not ideal for use in indoor environments because it necessitates an unobstructed view of the link connecting the GPS satellites and users (Ezhumalai et al., 2021; J. Wang & Park, 2021). In indoor environments, meeting this requirement is challenging because signals are often blocked by the thick walls of buildings, resulting in a weakened signal that diminishes the accuracy of indoor positioning data.

Pertaining to the above-mentioned issue, various wireless technologies such as Bluetooth, RFID, geomagnetism, proximity sensor, ultra-wideband (UWB), visible light, and Wi-Fi have been

DOI: 10.4018/JCIT.355244

This article published as an Open Access article distributed under the terms of the Creative Commons Attribution License (<http://creativecommons.org/licenses/by/4.0/>) which permits unrestricted use, distribution, and production in any medium, provided the author of the original work and original publication source are properly credited.

extensively studied for their applications to facilitate indoor positioning systems (Ezhumalai et al., 2021; J. Wang & Park, 2021). Among the available approaches, the fingerprinting method based on received signal strength (RSS) is unique because it does not need any additional infrastructure other than the commonly placed Wi-Fi access points (APs) or Bluetooth low energy (BLE) beacons, along with mobile devices equipped with network interface cards to measure RSS (Ezhumalai et al., 2021; Khalajmehrabadi et al., 2017a). Fingerprint-based indoor positioning using RSS measurements faces limitations due to the complexities of Wi-Fi signal propagation indoors. Multipath interference caused by reflections from walls, furniture, and even people disrupt the direct signal path, leading to unreliable RSS values and hindering radio map accuracy (Ji et al., 2022). Additionally, environmental factors like temperature and humidity can subtly affect signal strength, while human movement during measurements and device orientation can introduce further inconsistencies. These limitations can create significant discrepancies between the user's actual location and the estimated position based on RSS fingerprints.

The fingerprinting method based on RSS encompasses two main processes: the offline phase and the online phase. The offline phase is the process where the RSS measurements are taken from nearby APs at various reference points (RPs) throughout the indoor environment of interest to create a radio map containing the location-tagged RSS measurements (Shang & Wang, 2022). Specifically, Wi-Fi APs bridge wired networks (Ethernet) with Wi-Fi devices using radio frequencies for data transmission and reception. Meanwhile, a RP is a specific location within the indoor environment where RSS measurements are taken. These measurements capture the unique "fingerprint" of the Wi-Fi signal at that particular point. On the other hand, in the online phase, the user's unknown location can be approximated by comparing the RSS values obtained from visible APs near the user's current location with the labeled RSS vectors pre-collected and stored in the radio map, using a localization technique such as decision tree, random forest, or k -nearest neighbor (KNN; Ezhumalai et al., 2021; J. Wang & Park, 2021).

However, generating the radio map can be a time-consuming and labor-intensive process since it requires the RSS measurements to be performed at each RP defined over the entire indoor environment (Bi et al., 2018). Taking the real-world scenario, which usually involves a large-scale multi-floor indoor environment, would imply that a more significant number of RPs must be defined to cover the whole area of interest. Apart from that, to suppress the adverse effect introduced by outliers and noises, it is common to calculate and store the average RSS vectors as fingerprints in the radio map by collecting multiple measurements at each RP. Additionally, in some cases, multiple directional sampling is performed at each RP to account for the influence of human body shielding on RSS measurements.

In view of that, it would indeed be more labor- and time-efficient if the RSS is only measured at a coarser granularity than that of the RPs. However, to achieve a more accurate indoor positioning result, it would be beneficial to define as many RPs as possible in the indoor environment of interest and to collect more RSS fingerprints of those densely established RPs so that a more accurate radio map could be created. Thus, interpolation could be used to be more labor- and time-efficient while establishing sufficient RPs to construct a better radio map. This approach leverages a strategically chosen, sparse set of RPs with meticulously measured RSS fingerprints. These measurements form the basis of a preliminary radio map. Subsequently, a dense grid of virtual points (VPs) is defined across the indoor space. Interpolation techniques, such as inverse distance weighted (IDW; D. Wang et al., 2019) or kriging (Jan et al., 2015), then estimate the RSS fingerprints for each VP based on the known RSS values from the RPs. This process effectively creates an interpolated radio map. By combining this interpolated map with the initial radio map generated from physical measurements, a more detailed representation of the environment is achieved. This potentially reduces radio map creation effort while maintaining or even improving positioning accuracy due to the increased spatial resolution of the interpolated VPs.

While numerous radio map interpolation techniques exist, the existing literature predominantly adopts a uniform distribution of known RPs. However, such uniform density of known RPs across

all zones may not be optimal in scenarios where certain zones necessitate a higher density of known RPs. For instance, zones located farther away from APs or those experiencing significant RSS attenuation due to indoor layout intricacies may suffer from reduced localization performance. To address this limitation, this paper proposes an RSS-based optimization technique for an improved radio map interpolation. The density of known RPs allocated in each zone is varied according to the number of APs in which their average RSS exceeds the threshold RSS. The more the number of APs whose average RSS exceeds the threshold RSS set, the lower the density of known RPs that will be allocated to that zone, and vice versa. After collecting the RSS data from various APs in an indoor environment, the next step is to interpolate the RSS values at VPs using the IDW interpolation method. This process results in an interpolated radio map that is combined with the initial radio map to create an updated radio map. The updated radio map is then used in conjunction with the KNN localization scheme for indoor positioning. In this context, KNN searches a pre-built radio map for the k most similar RPs based on their RSS fingerprints. User location is estimated using a weighted average (or similar technique) of these KNNs' positions. In essence, KNN performs a similarity-based localization, with closer neighbors having a stronger influence. By increasing the density of known RPs in zones with poor AP coverage, the quality of the radio map and, consequently, localization performance in those areas can be significantly improved.

For brevity, the contributions of this work can be summarized.

1. A novel RSS-based optimization technique for improved radio map interpolation is proposed to enhance the localization performance by adjusting the density of known RPs based on the number of APs with an average RSS exceeding the threshold.
2. A rigorous performance evaluation is performed to validate the effectiveness of the proposed RSS-based radio map interpolation technique. By using a real-world hybrid Wi-Fi and BLE data set collected in a multi-story building, the performance of the proposed scheme is benchmarked against the existing IDW approach, which employs uniform distribution of known RPs. To provide a comprehensive analysis, the performance of the techniques in consideration are assessed using various key performance metrics, such as average positioning error and performance gain, along with scrutiny of spatial distribution of positioning errors.
3. A comprehensive analysis is conducted to assess and analyze the performance of both the proposed and baseline techniques in indoor environments with different placement and number of APs. Furthermore, the discussion encompasses insights into implementation cost, computational complexity, and execution time required for both approaches. Notably, our results reveal that the proposed method achieves an overall improvement of at least 3.70% in terms of average positioning error over the existing approach in various scenarios considered.

Following the introduction are the remaining five sections of this paper: Section 2 provides a survey of previous research on radio map interpolation, with Section 3 detailing the IDW interpolation algorithm. Section 4 outlines the optimization approach proposed for RSS-based radio map interpolation. In Section 5, we present the results of our performance evaluation and discuss the findings. Finally, Section 6 provides concluding remarks.

RELATED WORKS

Various interpolation algorithms have been utilized by researchers to reduce the time and labor required to construct radio maps. For instance, Kiring et al. (2020) employed the IDW and KNN interpolation algorithms in their study, evaluating the interpolation errors by calculating the root mean square error between the actual and estimated RSS measurements, both with and without spatial correlation, for different sparsity parameters (i.e., the probability of retaining RSS measurements in the radio map).

It seems that a comprehensive study on the performance of various interpolation and extrapolation methods was conducted in Talvitie et al. (2015). Specifically, IDW, linear interpolation, minimum method extrapolation, mean method extrapolation, gradient method extrapolation, and nearest neighbor are evaluated over different percentages of removed RSS fingerprints. The study investigated the average RSS estimation error for each method, while varying the percentage of interpolated RSS fingerprints. The accuracy of indoor positioning was compared among four different methods: the original fingerprint, incomplete fingerprint (without interpolation), interpolated fingerprint, and a combined interpolated and extrapolated fingerprint, with respect to their performance.

Bi et al. (2018), on the other hand, proposed a radio map construction via crowdsourcing and interpolation. Crowdsourcing was first adopted to collect the RSS fingerprints for a small number of RPs using different devices. To take the device heterogeneity issue into account, normalization was performed subsequently. The RSS fingerprints for the interpolated points were then calculated with the aid of the IDW interpolation algorithm. Apart from that, dimensionality reduction of the radio map was also performed using the principal components analysis algorithm to reduce the computational complexity.

Moreover, to construct a radio map for the experiment testbed that includes inaccessible areas where measurement of RSSs would be hindered, a kriging-based interpolation, which exploited the correlation of the spatial distribution of RSS, was presented by Zuo et al. (2018). Due to the existence of spatial correlation, which refers to the attributes on a geographic surface that are related to each other, the RSS values at one location can be calculated based on the RSS values at several neighboring locations with the implicit assumption that closer points have a more substantial influence on each other compared to the influence contributed by distant points.

In Zhao et al. (2016), the universal kriging (UK) method was used to interpolate the RSS values for the defined interpolation points. Virtual augmentation of the space boundary was also performed by establishing additional interpolation points beyond the original space. This is essential in overcoming the boundary effect, which usually results in the reduction of the positioning accuracy at the boundary. With the RSS fingerprints measured for only 28 known RPs, this technique can achieve an average positioning error comparable to that of when the RSS fingerprints are measured for 112 known RPs. A performance comparison was made between the IDW, ordinary kriging and UK (fitting and spherical models) interpolation methods.

Jan et al. (2015) initially recorded the RSS fingerprints at a limited number of RPs and then used the kriging algorithm to interpolate the RSS fingerprints at additional unobserved locations. They assessed the impact of varying the number of basic RPs and kriging RPs on the positioning error. Additionally, they evaluated the RSS interpolation error by contrasting the interpolated RSS fingerprints with the measured RSS fingerprints.

Furthermore, another approach presented in Racko et al. (2017) adopted linear and Delaunay interpolations to calculate the RSS fingerprints. Subsequently, the interpolation errors were obtained by comparing the interpolated RSS values with the actual RSS fingerprints collected beforehand. A performance comparison between the two interpolation techniques was also performed.

In Redondi (2018), a graph-based signal interpolation method for localization was presented. In this approach, RSS measurements were regarded as signals that are defined on a graph. In this graph, nodes correspond to physical locations, while edges correspond to distances between those locations. By utilizing the relationships between known nodes and known/unknown nodes, the method captures global information to estimate RSS values at unknown nodes. A comparison with traditional interpolation methods, such as IDW, radial basis function, and model-based interpolation, demonstrates that the graph-based signal interpolation method performs superiorly in terms of accuracy.

In Suto et al. (2021), a novel approach using image processing techniques was proposed for estimating the spatial distribution of RSS data. The methodology utilized in this study involved treating radio propagation data as an image and applying a deep learning (DL) framework to transform the spatial interpolation problem into a shadowing adjustment problem through the use of path loss

regression. A neural network structure was employed to solve the shadowing adjustment problem, using a gradual training method to ensure stability. This DL framework outperformed existing image-driven DL methods such as generative adversarial network-based models and spatial interpolation with a convolutional neural network.

In the crowdsourcing-based radio map construction approach proposed in Ye and Wang (2018), some specific grids in the indoor environment may have had too few or even no crowdsourced samples, which created a nonuniform spatial distribution issue due to the random and voluntary nature of the crowdsourcing approach. To address this problem, a binary polynomial function was utilized to interpolate additional RSS fingerprints based on the RSS fingerprints of neighboring grids for the grids with insufficient crowdsourced samples. To avoid incorporating distant grids, which could result in substantial variations in RSS and compromise the quality of the interpolated radio map, only a select number of grid distinct RSS fingerprints were chosen instead of considering all surrounding grids. The performance was evaluated for different ratios of deficiency grids and various ratios of outliers in the sufficiency grids.

The focus of the method described in Z. Wang et al. (2021) was to create a radio map for indoor localization by using an enhanced low-rank matrix completion technique. The method was based on the idea that the RSS data matrix in indoor environments has low-rank attributes. It involved measuring RSS fingerprints at a limited number of RPs and then using a low-rank matrix completion algorithm to fill in the remaining fingerprints in the radio map. To stabilize the solution and suppress the noise resulting from the environment and equipment, the Frobenius parameter was integrated into the low-rank matrix completion model.

With the least absolute shrinkage and selection operator based interpolation scheme proposed by Khalajmehrabadi et al. (2017b), a radio map could be reconstructed by the RSS fingerprints interpolation at a finer granularity based on the RSS fingerprints measured at a coarser granularity of RPs. Due to the sparse RSS fingerprints, the sparse recovery algorithm could be used for the sparse reconstruction of the radio map. An outlier detection scheme was introduced into the radio map interpolation procedure to suppress the impact of outliers and ensure that the RSS fingerprints of RPs used for interpolation were outlier free. The radio map reconstruction error, which represents the absolute difference between the actual and reconstructed radio maps, was also determined for different ratios of selected RPs.

The work in Bi et al. (2019) presented an adaptive path-loss model interpolation method. In this method, crowdsourcing was first performed to collect the RSS fingerprints at sparse RPs. Subsequently, for all visible APs, the path-loss models with optimal parameters estimated using the least squares method were formed with the aid of RPs in a small area. These path loss models were then utilized to compute the RSS fingerprints of the interpolation points. The performance of the adaptive path-loss model interpolation method was compared with that of the IDW and kriging interpolation methods for different sampling intervals of the sparse RPs. Nevertheless, this method has a drawback since it requires knowledge of the exact locations of the APs.

In Boujnah and Korbel (2016), a localization method that utilizes crowdsourcing, data clustering, and multidimensional interpolation was also presented. The method presented partitioned the data collected from crowdsourcing into smaller areas based on the cell identifiers of the received signal. If the number of partitions exceeded a threshold, k -means or fuzzy c -means clustering was employed to group the RSS fingerprints into clusters. The user's unknown location was then predicted by using the interpolation function for each cluster, which is determined by radial basis function with a Gaussian kernel.

To overcome the limitations of radio map creation, researchers have explored diverse optimization techniques for interpolation, aiming to refine the process from multiple aspects. Tian et al. (2018) addressed the challenge of achieving optimal radio map creation by investigating fingerprint reporting for WLAN localization accuracy. The authors demonstrated that the fingerprint reporting optimization problem is NP-hard (nondeterministic polynomial-time) and proposed a novel algorithm

that achieved near-optimal accuracy with sufficient data. The proposed method tackled the issue of similar fingerprints for distant and nearby locations, leading to improved overall positioning accuracy. Furthermore, the relationship between location accuracy and Wi-Fi signal coverage was explored for optimal AP deployment. Their theoretical analysis was validated through experimentation. Additionally, the work in Nabati et al. (2020) investigated the use of pattern recognition algorithms for optimizing user location. Traditional methods in this field train on separate x and y coordinates, neglecting the inherent two-dimensional nature of signal fingerprints. To address this limitation, the authors proposed a novel two-dimensional Gaussian process regression (GPR) method that optimized accuracy by jointly using x and y information during training with a specialized PRA-based GPR. This method achieved significant improvements ($>40\text{cm}$) in accuracy with less data and lower computational cost compared to conventional GPR.

Subsequently, a 5G fingerprinting system for indoor positioning achieved significant accuracy improvement through optimization. The system employed Kalman filtering to pre-process raw data and utilized UK for optimized database creation via spatial interpolation (Huang et al., 2021). KNN then pinpointed user location. Experiments demonstrated positioning accuracy improvements of 53% and 43% in two test rooms, with a best-case error of 1.44 meters for 80% of samples. Moreover, the work in Huo et al. (2021) presented a low-cost, long-life fingerprint localization system for indoor rooms using IEEE802.15.4 devices. To address signal fluctuations, the authors proposed a parameter optimization method that assigned and optimized multiple fingerprints per room. Huo et al. (2022) proposed an improved fingerprint optimization method for FILS15.4, an indoor localization system using low-power IEEE802.15.4 devices. The method addressed signal fluctuations by assigning and optimizing multiple fingerprints per room, leading to significant accuracy improvements ($>97\%$) validated in a real-world testbed.

Although previous research has explored how the quantity of known RPs affects interpolation, there has been limited focus on optimizing the density of known RPs. Ezpeleta et al. (2015) employed various interpolation methods, including Euclidean distance linear basis, multi-quadratic, thin plate spline, and polyharmonic spline functions, to compute the RSS fingerprints for the interpolated points in their study. Furthermore, they analyzed the impact of the density and distribution of known RPs on indoor localization error. Unlike other studies, they assumed that RF signal quality is better for locations closer to the beacons, leading to variation in the density of known RPs. Consequently, regions in proximity to the beacons were designated a reduced density of known RPs, whereas those further away were allocated a higher density.

RADIO MAP INTERPOLATION

Construction of Initial Radio Map

During the offline phase, the RSS readings from D APs at each of the M predefined RPs are measured. Subsequently, the radio map χ is constructed by storing all the location labeled RSS fingerprints and it can be expressed as shown in Equation 1.

$$\chi = \begin{bmatrix} (l_{1,1} & l_{1,2} & \cdots & l_{1,Q}) & (r_{1,1} & r_{1,2} & \cdots & r_{1,D}) \\ & \vdots & & & & \vdots & & \\ (l_{m,1} & l_{m,2} & \cdots & l_{m,Q}) & (r_{m,1} & r_{m,2} & \cdots & r_{m,D}) \\ & \vdots & & & & \vdots & & \\ (l_{M,1} & l_{M,2} & \cdots & l_{M,Q}) & (r_{M,1} & r_{M,2} & \cdots & r_{M,D}) \end{bmatrix} \quad (1)$$

In Equation 1, $\chi \in \mathbb{R}^{M \times (Q+D)}$, $l_m = [l_{m,1} \ l_{m,2} \ \dots \ l_{m,Q}]^T$ is the location identifier vector for the m -th RP, Q denotes the total number of location identifiers utilized to define each RP, $r_m = [r_{m,1} \ r_{m,2} \ \dots \ r_{m,D}]^T$ indicates the RSS fingerprint vector at the m -th RP, $r_{m,d}$ signifies the RSS from AP d at the m -th RP, $m \in [1, M]$ and $d \in [1, D]$. (1) can also be expressed more concisely as shown in Equation 2.

$$\chi = [L \ R] \quad (2)$$

In Equation 2, $L = [l_1 \ l_2 \ \dots \ l_M]^T \in \mathbb{R}^{M \times Q}$ and $R = [r_1 \ r_2 \ \dots \ r_M]^T \in \mathbb{R}^{M \times D}$.

Meanwhile, during the online phase, machine learning technique is invoked to predict the position of the user by matching the RSS fingerprint measured at the unknown position $ur_u = [r_{u,1} \ r_{u,2} \ \dots \ r_{u,D}]^T$ with the RSS fingerprints stored on the radio map. Since the radio map quality plays a critical role in governing the positioning performance, it is thus common to enhance the localization performance by increasing the density of the RPs. Nevertheless, certain drawbacks, such as the labor-intensive and time-consuming RSS fingerprint collection process, are often associated with such an act. Hence, to ensure reliable localization while simultaneously being labor and time savvy, it is essential to build an improved interpolated radio map with an optimized zone-based density of RPs so that the density of RPs is increased effectively at only necessary zones with poor localization performance.

Generation of Virtual Points Through Inverse Distance Weighted Interpolation

IDW interpolation is a deterministic method used for spatial interpolation. The IDW interpolation technique estimates the value of an unknown location by determining a weighted average of the known values within its proximity. The assigned weights to the known values are dependent on their distance from the unknown location, and the calculated weighted average is utilized to approximate the value at the unknown location. Applying the IDW interpolation algorithm for the radio map construction in indoor positioning, the RSS values from the d -th AP at the u -th VP which is represented by $r_{u,d}$ can be evaluated based on the values of RSS of the N nearest known RPs using Equation 3.

$$r_{u,d} = \frac{\sum_{i=1}^N w_i \tilde{r}_{i,d}}{\sum_{i=1}^N w_i} \quad (3)$$

In Equation 3, u refers to the index of the VPs, i denotes the index of the N nearest known RPs, $\tilde{r}_{i,d}$ is the RSS of the d -th AP at the i -th nearest known RPs that is selected from the d -th column of R , and w_i signifies the interpolation weight which can be expressed as shown in Equation 4.

$$w_i = \frac{1}{d_{(u,i)}^\alpha} \quad (4)$$

In Equation 4, $d_{(u,i)}$ represents the Euclidean distance between the u -th VP and the i -th nearest known RP. More specifically, the power exponent α , which is a user-determined parameter, dictates the rate at which the weight of each known RP decreases as the distance between the virtual point and the RP increases. From Equations 3 and 4, it is apparent that a higher α value will cause the weights for distant points to decay more rapidly and the nearby RPs to have greater influence on the interpolated RSS of the VP.

In the IDW interpolation, each point has a local influence on the predicted value that diminishes with distance. To be more specific, IDW interpolation assigns greater weights to points that are closer to the interpolated location compared to those that are farther away. Only the N nearest neighbors,

which refers to a specified number of points closest to the interpolation location, participate in calculating the predicted value of the interpolation location.

PROPOSED TECHNIQUE

In the baseline technique, each floor is split evenly into Z zones such that each zone has the same density of known RPs. Apart from that, the known RPs and VPs also follow a uniform distribution across all zones.

Nevertheless, such a uniform density of known RPs across all zones might not be optimal for situations whereby certain zones would generally require a higher density of known RPs than other zones. For instance, consider a situation whereby certain zones are located farther away from the APs, and thus the RSS measured for the RPs in those zones might possess a lower quality, and this will adversely affect the accuracy of user location prediction at these zones. As such, Ezpeleta et al. (2015) proposed a method to vary the density and distribution of the known RPs according to the distance of the zones from the beacons. However, they only considered a relatively straightforward single-floor testbed in their investigation whereby the beacons are densely gathered around a particular zone, whereas the other zones are far apart from the beacons. Nevertheless, in a multi-floor testbed, it is possible for a zone to be located far away from APs on the same floor but located near to APs on the floor directly above or below it. Thus, to tackle this issue, an optimization technique for RSS-based radio map interpolation was proposed to vary the density of the known RPs in each zone instead.

The flowchart for the proposed optimization technique for RSS-based radio map interpolation is depicted in Figure 1 below. First, each floor is split evenly into Z zones and G known RPs are selected as the delegate known RPs in each zone. Subsequently, for each AP present on the floors of the area of interest, the average RSS of these G delegate known RPs measured from that AP is calculated and checked to see whether it exceeds the threshold of the RSS t fixed. The average RSS of G delegate known RPs in zone z of floor f measured from AP d is denoted as $\beta_{f,z}^d$, and it can be expressed as shown in Equation 5.

$$\beta_{f,z}^d = \frac{\sum_{g=1}^G RSS_{f,z,g}^d}{G} \quad (5)$$

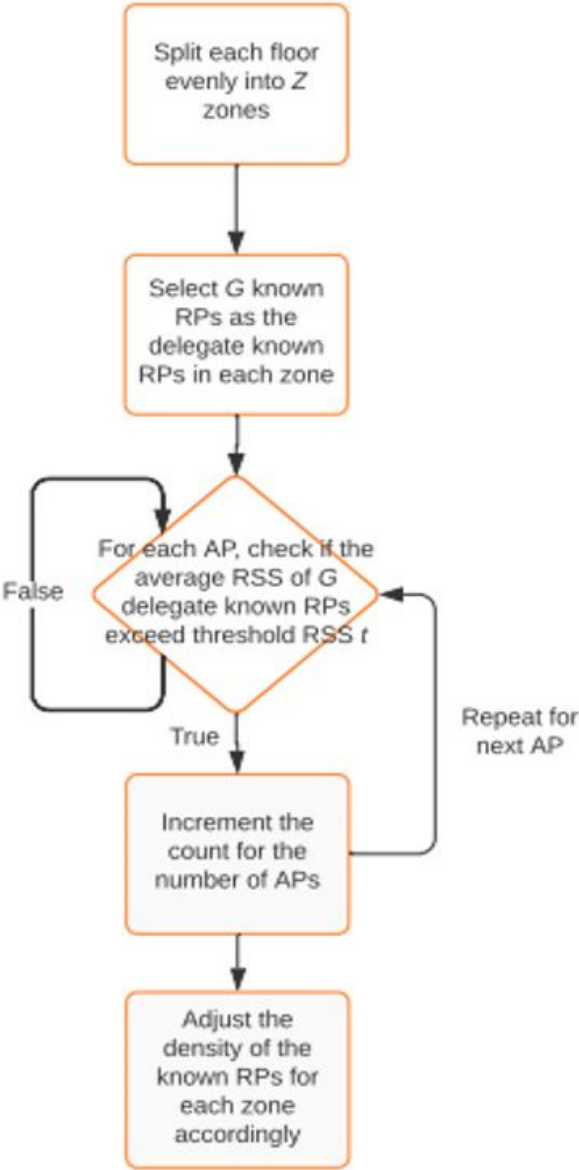
In Equation 5, $f = 1, 2, \dots, F$, $z = 1, 2, \dots, Z$, $g = 1, 2, \dots, G$, $d = 1, 2, \dots, D$, and $RSS_{f,z,g}^d$ is the RSS measured from AP d at delegate known RP g located at zone z of floor f .

If $\beta_{f,z}^d > t$, then the count for the number of APs for zone z in floor f , which is represented as $\kappa_{f,z}$ would be incremented by one. The density of known RPs allocated to zone z of floor f can be expressed as shown in Equation 6.

$$\gamma_{f,z} = \begin{cases} \delta_1 & \text{if } 0 \leq \kappa_{f,z} \leq \eta_{f,1} \\ \delta_2 & \text{if } \eta_{f,1} < \kappa_{f,z} \leq \eta_{f,2} \\ \vdots & \vdots \\ \delta_S & \text{if } \eta_{f,S-1} < \kappa_{f,z} \leq \eta_{f,S} \end{cases} \quad (6)$$

In Equation 6, $\delta_1 > \delta_2 > \dots > \delta_{S-1} > \delta_S > 0$, $0 < \eta_{f,1} < \eta_{f,2} < \dots < \eta_{f,S-1} < \eta_{f,S}$, $\eta_{f,S}$ and S indicate the switching threshold and a total number of switching thresholds for each floor, respectively. More explicitly, zones with a higher number of APs exceeding the threshold have a lower density of known RPs. Conversely, zones with fewer APs above the RSS threshold have a higher density of known RPs. The rationale for this strategy is that the zones with fewer APs meeting the threshold

Figure 1. Flowchart for the proposed optimized RSS-based radio map interpolation technique



typically perform worse than those with more APs above the threshold. By allocating more known RPs to these underperforming zones, the localization performance in these zones can be enhanced. Nevertheless, the global density of the known RPs for each floor remains constant, as shown in Equation 7. To guarantee a fair evaluation of the proposed and baseline techniques, H denotes the total number of known RPs for each floor.

$$\gamma_f = \sum_{z=1}^Z \gamma_{f,z} = H \tag{7}$$

Next, the interpolated RSS values for the VPs are computed using IDW interpolation. The resulting interpolated RSS map is combined with the initial radio map, which includes the RSS values for the known RPs, to create an updated radio map. The KNN localization algorithm is then used to predict the indoor location of the validation samples based on this updated radio map. KNN is selected for location prediction due to its simplicity and ease of implementation. During real-time localization, KNN identifies the k -nearest neighboring RPs by computing the Euclidean distance between the RSS data collected online and the reference fingerprint in the radio map. The estimated coordinate of the unknown target is then calculated using the center of mass of these neighboring points.

RESULTS AND ANALYSIS

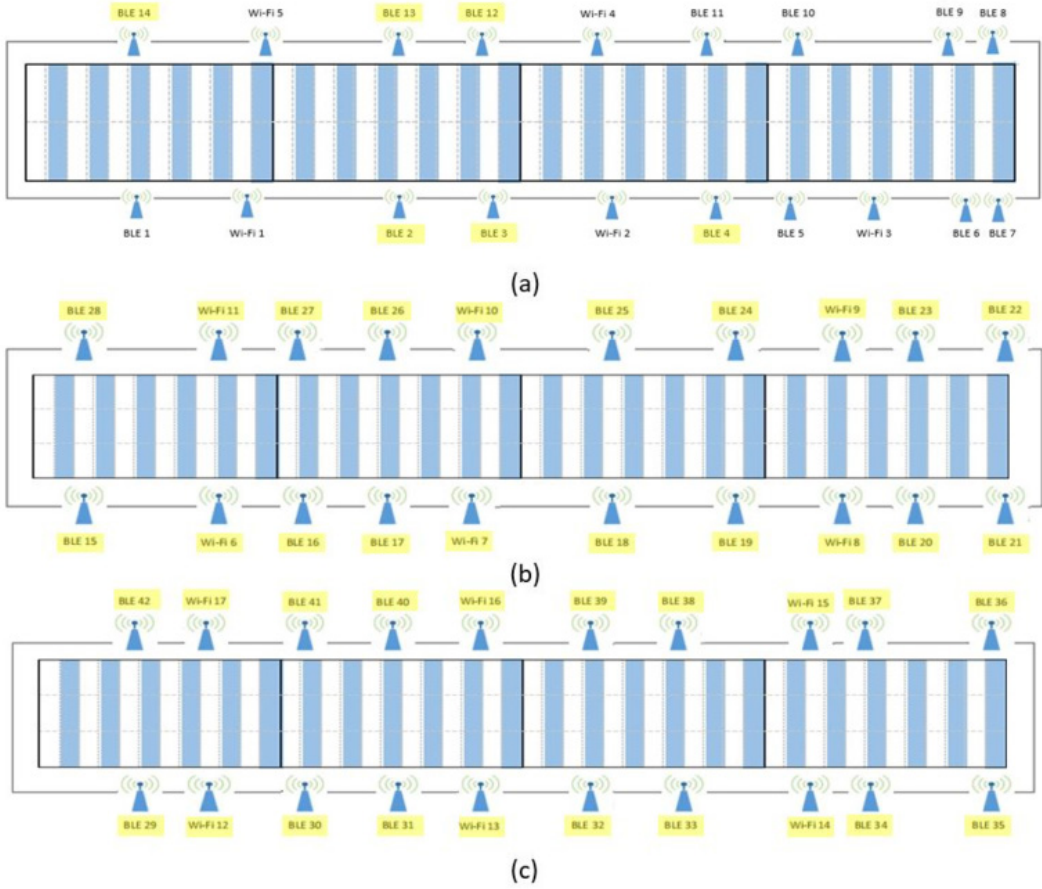
Simulation Setup

The hybrid fingerprint data with layout change (HDLC; Nor Hisham et al., 2022)—gathered from the ground, first, and second floors of the Faculty of Engineering, Wing B building, at the Multimedia University Cyberjaya campus—was utilized in this study to assess the efficacy of the proposed technique and compared with that of the baseline technique. The HDLC data set contains a total of 11,520 samples, whereby 7,680 instances are the training samples while the remaining 3,840 instances are the testing samples. Among the 7,680 instances, 1,920 instances are recorded for the ground floor, 2,880 instances are recorded for the first floor, and the remaining 2,880 instances are recorded for the second floor. There is a total of 96 RPs distributed across the ground floor, while there are 144 RPs each for the first floor and also the second floor. For each RP, 20 samples were collected to construct the training data set, while for each test point (TP), 10 samples were collected to build the testing data set. The HDLC data set comprises 62 attributes, including BLE and Wi-Fi fingerprints for 42 beacons and 17 Wi-Fi routers, respectively, as well as x-coordinates, y-coordinates, and floor number. The RSS intensity values are expressed as negative values within the range of -110 dBm to -36 dBm.

Each floor was partitioned evenly into four zones. Rows 0 to 11 represent Zone 1, rows 12 to 23 represent Zone 2, rows 24 to 35 represent Zone 3, whereas rows 36 to 47 represent Zone 4. To assess the effectiveness of the proposed technique, the performance of the proposed RSS based radio map interpolation technique was benchmarked against the baseline IDW method, which uniformly allocates known RPs across all zones. For the baseline technique, each zone is allocated with 50% of the uniformly distributed known RPs while the remaining 50% is defined as the VPs. As for the proposed technique, 25% of the points in each zone were selected uniformly as the delegate known RPs. Depending on the number of APs in which their average RSS of the G delegate known RPs exceeds the threshold RSS t , the zone-based density of the known RPs is higher or lower than 50% and the distribution of the known RPs is no longer uniform. Nevertheless, the total number of known RPs distributed across four zones of the floor would be kept constant for both the baseline and proposed technique. To achieve this, the total percentage increase in the density of known RPs for certain zones would imply the total percentage decrease in the density of known RPs that other remaining zones on the same floor would need to bear. Consequently, the implementation cost, including labor effort and time, required for collecting the known RPs, is identical for both the proposed and baseline techniques. Improved localization could be achieved by increasing the number of known RPs, albeit at a higher implementation cost.

Figures 2 and 4 depict the density and distribution of known RPs in all four zones for the baseline technique in Scenarios 1 and 2, respectively. On the other hand, Figures 3 and 5 show the same for the proposed technique in both scenarios. To demonstrate the efficacy of the proposed technique, two scenarios were devised. In Scenario 1, some of the APs on the ground floor are silenced, while the remaining APs on the first and second floors are left active. Conversely, in Scenario 2, only the APs on the 1st floor remain active, while some of the APs on the ground and second floors are silenced. The APs kept intact are highlighted in yellow as shown in Figures 2 to 5. Note that the blue cells denote the VPs, white cells denote the known RPs, and pink cells denote the delegated known RPs.

Figure 2. Density and distribution of known RPs for baseline technique in scenario 1: (a) ground floor; (b) first floor; (c) second floor



The proposed technique and the baseline technique are compared in regard to the average positioning error on a zone-based, floor-based, and overall basis. The average positioning error “a” is computed by determining the Euclidean distance between the predicted coordinates $(\hat{x}_i, \hat{y}_i) = [(\hat{x}_1, \hat{y}_1), (\hat{x}_2, \hat{y}_2), \dots, (\hat{x}_M, \hat{y}_M)]$ and the actual coordinates $(x_i, y_i) = [(x_1, y_1), (x_2, y_2), \dots, (x_M, y_M)]$ as given in (8) where M is the total number of RPs/instances in the radio map, as shown in Equation 8.

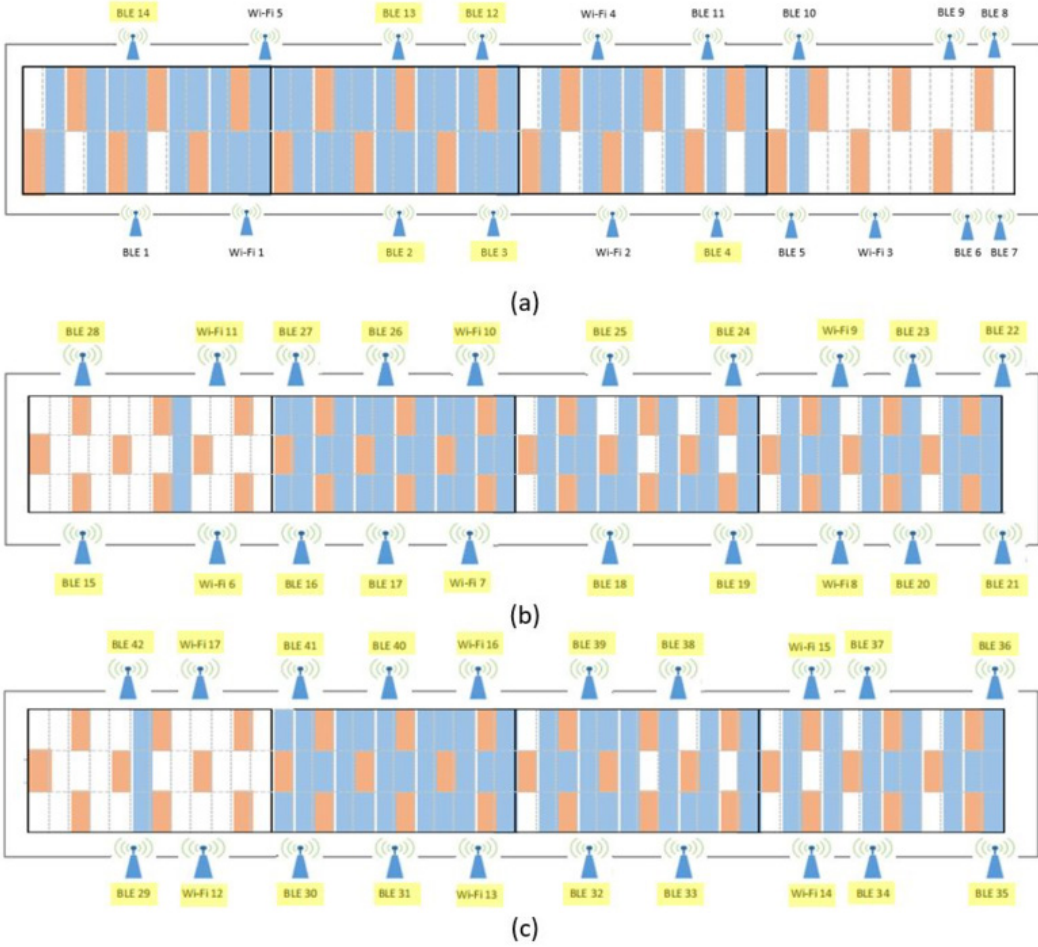
$$a = \frac{\sum_{i=1}^M \sqrt{(\hat{x}_i - x_i)^2 + (\hat{y}_i - y_i)^2}}{M} \quad (8)$$

Additionally, the performance gain P_ϵ of the proposed system over the baseline scheme in terms of average positioning errors is also presented in this work and is computed using Equation 9.

$$P_\epsilon = \frac{\epsilon_B - \epsilon_R}{\epsilon_B} \times 100\% \quad (9)$$

In Equation 9, where ϵ_B and ϵ_R signify the average positioning errors of the baseline and proposed techniques, respectively. Further, to provide an in-depth analysis on the localization performance for

Figure 3. Density and distribution of known RPs for proposed technique in scenario 1: (a) ground floor; (b) first floor; (c) second floor



each RP, the differences in positioning errors between baseline and proposed techniques for each RP can be computed using Equation 10.

$$\Delta_{f,i} = \varepsilon_{f,i}^B - \varepsilon_{f,i}^R \quad (10)$$

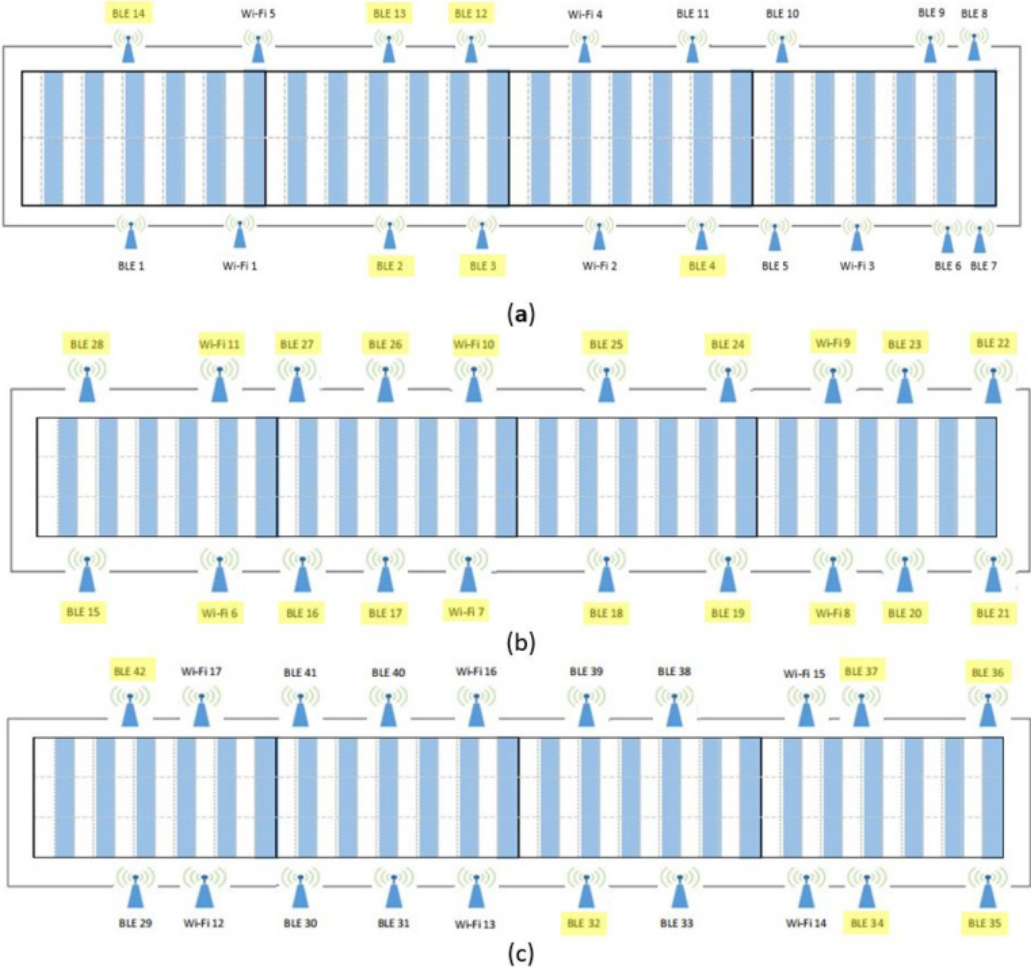
In Equation 10, where $\Delta_{f,i}$ represents the difference in positioning errors between the baseline and proposed techniques for i -th RP on floor f , $\varepsilon_{f,i}^B$ and $\varepsilon_{f,i}^R$ denote the positioning errors of the baseline and proposed techniques for i -th RP on floor f , respectively.

Results and Discussions

To assess the effectiveness of the proposed optimized technique for radio map interpolation based on RSS, a zone-level analysis was conducted for each floor. Additionally, a floor-level analysis and an overall analysis for all three floors were also conducted. For all scenarios, the hyperparameter for the IDW algorithm is selected as 10 nearest neighbors ($n=10$).

According to the proposed optimized RSS-based radio map interpolation technique, the more the number of APs in which their average RSS of the G delegated known RPs exceeds the threshold

Figure 4. Density and distribution of known RPs for baseline technique in scenario 2: (a) ground floor; (b) first floor; (c) second floor



RSS t set, the lower the density of known RPs that is allocated to that zone. For an AP’s RSS to be deemed usable for positioning, it must exceed the noise floor, which is typically around -100 dBm, to ensure that the user device is able to distinguish between signal and noise. As such, the threshold RSS t is set as -85 dBm throughout the entire simulation as it ensures that the RSSs are sufficiently above the noise floor and represents the minimum signal strength required for basic connectivity. Thus, Table 1 shows the number of APs with average RSS of the G delegate known RPs that exceeds -85 dBm in each zone for Scenarios 1 and 2. Consequently, the new density of known RPs allocated to the zones of the floors for Scenarios 1 and 2 is also listed in Table 1.

After determining the density of known RPs assigned to each zone of every floor as presented in Table 1 and their distribution illustrated in Figures 3 and 5, the KNN localization algorithm with $K = 2$ is trained for indoor location prediction using the newly created radio map through interpolation. Since the sum of known and interpolated RPs in the final radio map is the same for both the proposed and baseline techniques, and all techniques employ the same machine learning algorithm for positioning, the computational complexity and execution time for location prediction are identical across all techniques.

Figure 5. Density and distribution of known RPs for proposed technique in scenario 2: (a) ground floor; (b) first floor; (c) second floor

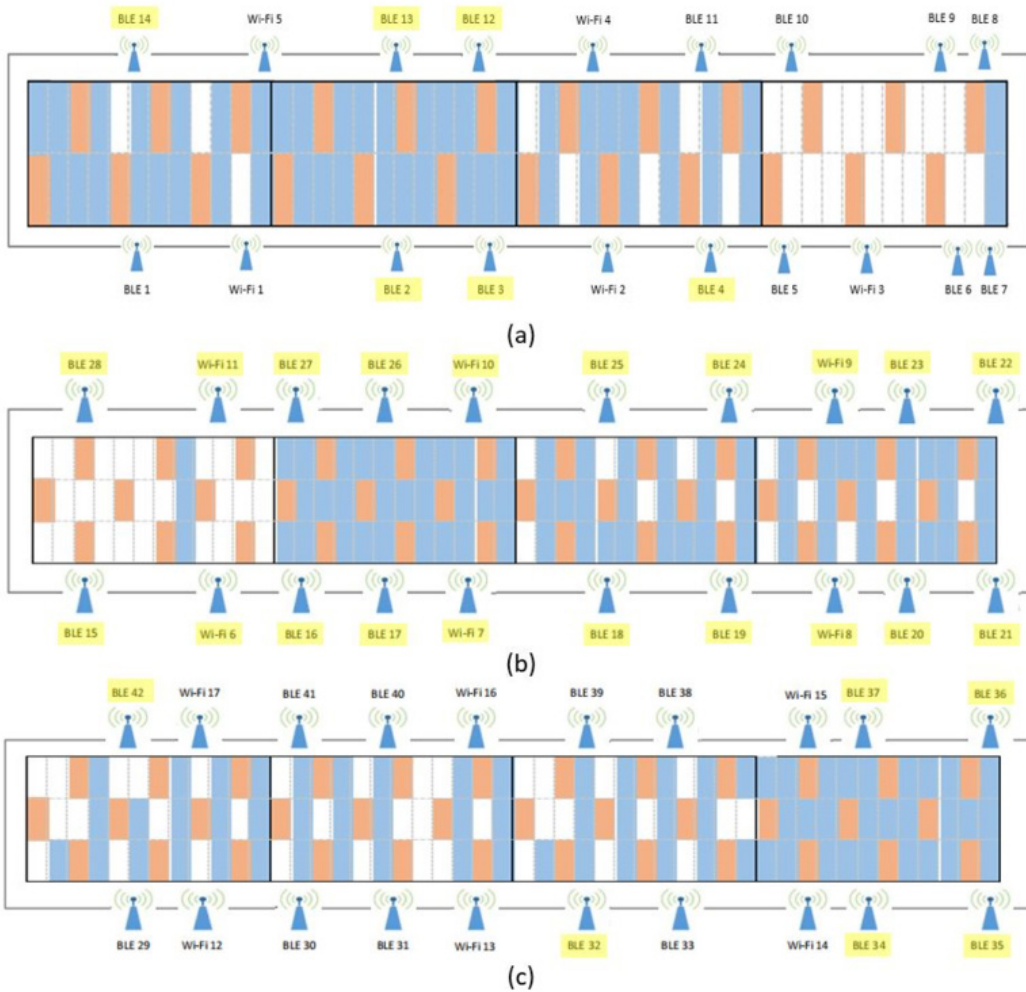


Table 2 presents a comparison of the average positioning error and performance gain between the baseline technique and the proposed technique for both scenarios.

Moreover, the average positioning error and performance gain for Scenarios 1 and 2 are also simulated for the ground, first, and second floors and all three floors. The results are as tabulated in Table 3.

From Table 1, it is observed for Scenario 1 that the zones on the ground floor have fewer number of APs in which their average RSS of the 25% delegate known RPs exceeds the threshold RSS t set, which is -85 dBm as compared to the zones located on the first and second floors. This is because all the APs on the first and second floors are left intact while most of the APs on the ground floor are muted. Likewise, for Scenario 2, where most of the APs on the ground and second floors are muted, the number of APs in which their average RSS of the 25% delegate known RPs exceeds -85 dBm for zones on the ground and second floors are much lower compared to that of the first floor, which has all of its APs kept intact. Hence, according to the proposed optimized RSS-based radio map interpolation technique, the density of known RPs assigned to the zones of each floor decreases as the number of APs whose average RSS exceeds -85 dBm increases for both scenarios.

Table 1. Known RP density settings for each zone of each floor according to the number of APs with average RSS of the delegate known RPs exceeding the threshold RSS for both scenarios

Floor	Zone	Number of APs		Known RPs Density (%)	
		Scenario 1	Scenario 2	Scenario 1	Scenario 2
0	1	3	3	37.5	37.5
	2	4	4	25	25
	3	1	1	46	46
	4	0	0	92	92
1	1	7	7	92	92
	2	13	13	25	25
	3	11	11	42	42
	4	11	11	42	42
2	1	7	1	92	58
	2	12	1	25	58
	3	11	1	39	58
	4	10	4	44	25

Note. AP=access point, RP=reference point

Table 2. Average positioning error and performance gain for each zone of each floor for both scenarios

Floor	Zone	Average Positioning Error (m)				Performance Gain (%)	
		Scenario 1		Scenario 2		Scenario 1	Scenario 2
		Baseline	Proposed	Baseline	Proposed		
0	1	1.8514	1.9432	1.8395	1.8003	-4.96	2.13
	2	1.7129	1.5312	1.7289	1.5362	10.61	11.15
	3	1.8747	1.7824	1.9977	1.9907	4.92	0.35
	4	3.7891	3.6056	3.9910	3.7091	4.84	7.06
1	1	2.0985	1.8865	2.1607	2.0425	10.10	5.47
	2	1.8203	1.8032	1.8570	1.8675	0.94	-0.57
	3	2.0674	2.2091	2.1615	2.0779	-6.85	3.87
	4	1.8970	1.9095	1.9896	1.8996	-0.66	4.52
2	1	2.1551	2.0215	2.0178	2.0278	6.20	-0.50
	2	1.8755	1.8583	1.8502	1.7783	0.92	3.89
	3	2.1737	2.1251	2.0536	2.0355	2.24	0.88
	4	1.9775	2.0095	2.2177	2.3285	-1.62	-5.00

Meanwhile, Table 2 demonstrates that the majority of zones on each floor exhibit a noticeable percentage of improvement in average positioning error for both scenarios. For Scenario 1, the average positioning error of those zones with the lowest number of APs whose average RSS exceeds -85 dBm improves rather significantly (4.84%, 10.10%, and 6.20% for Zone 4 on the ground floor, Zone 1 on the first floor, and Zone 1 on the second floor, respectively) when the proposed technique is implemented. A similar trend is also observed for Scenario 2, where the average positioning error

Table 3. Average positioning error and performance gain for each floor and as an overall for both scenarios

Floor	Average Positioning Error (m)				Performance Gain (%)	
	Scenario 1		Scenario 2		Scenario 1	Scenario 2
	Baseline	Proposed	Baseline	Proposed		
0	2.3381	2.1843	2.3654	2.2168	6.58	6.28
1	2.3326	2.2469	2.3548	2.2650	3.67	3.81
2	2.3632	2.3159	2.3788	2.3343	2.00	1.87
Overall	2.3455	2.2571	2.3665	2.2789	3.77	3.70

improves by 7.06% and 5.47% for Zone 4 on the ground floor and Zone 1 on the first floor, respectively. This phenomenon implies that those zones require a higher density of known RPs since they have insufficient strong APs for better performance of indoor location prediction as compared to the other zones in which the APs are more densely surrounded.

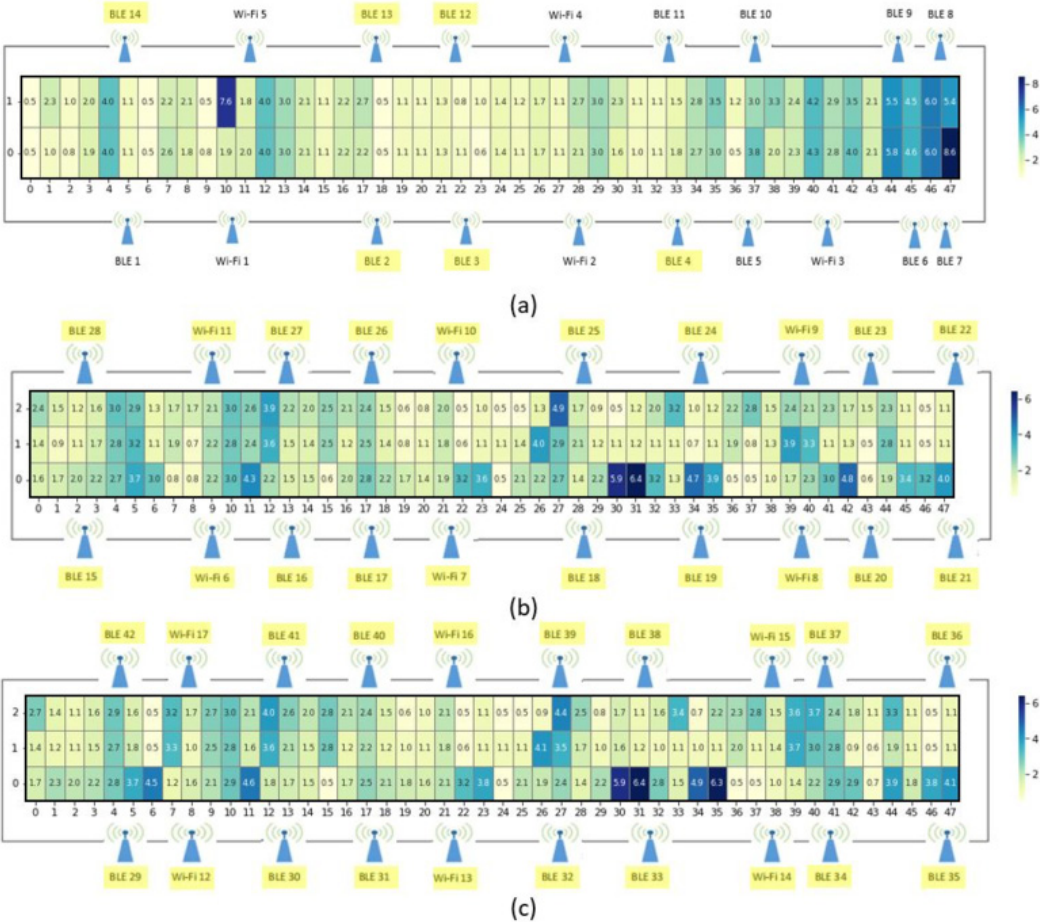
The heatmaps of the positioning errors for the ground, first, and second floors for the baseline and the proposed techniques are shown in Figures 6 and 7 for Scenario 1 and Figures 9 and 10 for Scenario 2. Meanwhile, Figures 8 and 11 show the heatmaps of the differences in positioning errors of the ground, first, and second floors between the baseline and the proposed techniques for Scenarios 1 and 2, respectively. Note that a positive value obtained for the positioning error implies an improvement in the proposed technique, while a negative value, on the other hand, implies a degradation in the positioning error with the proposed technique.

From Figure 6 (a), it is observed that for Scenario 1, the baseline technique performs poorly in Zone 4 of the ground floor as high positioning errors are concentrated in this area. This is attributed to the fact that Zone 4 has the least APs surrounding it compared to the other zones. Thus, Zone 4 is said to be isolated from all of the APs, and this results in a worse positioning error when baseline technique, which employs uniform zone-based density of known RPs, is implemented. Conversely, by allocating a higher density of known RPs to Zone 4 based on the number of APs whose average RSS of the designated known RPs surpasses the RSS threshold, the positioning errors for locations in this zone decrease. This trend could be observed from the heatmap shown in Figure 8 (a), where the majority of the locations in Zone 4 result in a positive positioning error difference, as implied by the blue gradients. Apart from that, Figure 8, (b) and (c), clearly indicates that the proposed technique exhibits superior localization performance compared to the baseline counterpart in term of positioning error for most locations within Zone 1 of the first and second floors, with only a few locations suffering from a minor degradation. As a result, a positive performance gain is obtained for the average positioning error of Zone 1 of the first and second floors.

Likewise, in Scenario 2, similar observations are made in Figure 9, (a) and (c), where the baseline technique results in higher positioning errors in Zone 4 on the ground floor and Zone 2 of the second floor due to fewer surrounding APs compared to other zones. From Figure 11, (a) and (c), it can be confirmed that the implementation of the proposed RSS-based interpolation optimization technique results in a positive positioning error difference in most of the locations found in Zone 4 of the ground floor and Zone 2 of the second floor. Besides, it is observed from Figure 11 (b) that most of the locations found in Zone 1 of the first floor experience an improvement in positioning error when comparing the baseline and proposed techniques. Therefore, a positive performance gain is obtained for the average positioning error of Zone 1 of the first floor.

Furthermore, the effectiveness of the proposed optimized RSS-based radio map interpolation technique is further underscored by the results presented in Table 3, which showcase improvements in average positioning errors for each floor, and overall, across all three floors, compared to the baseline technique in both scenarios. For Scenario 1, the average positioning errors for the ground,

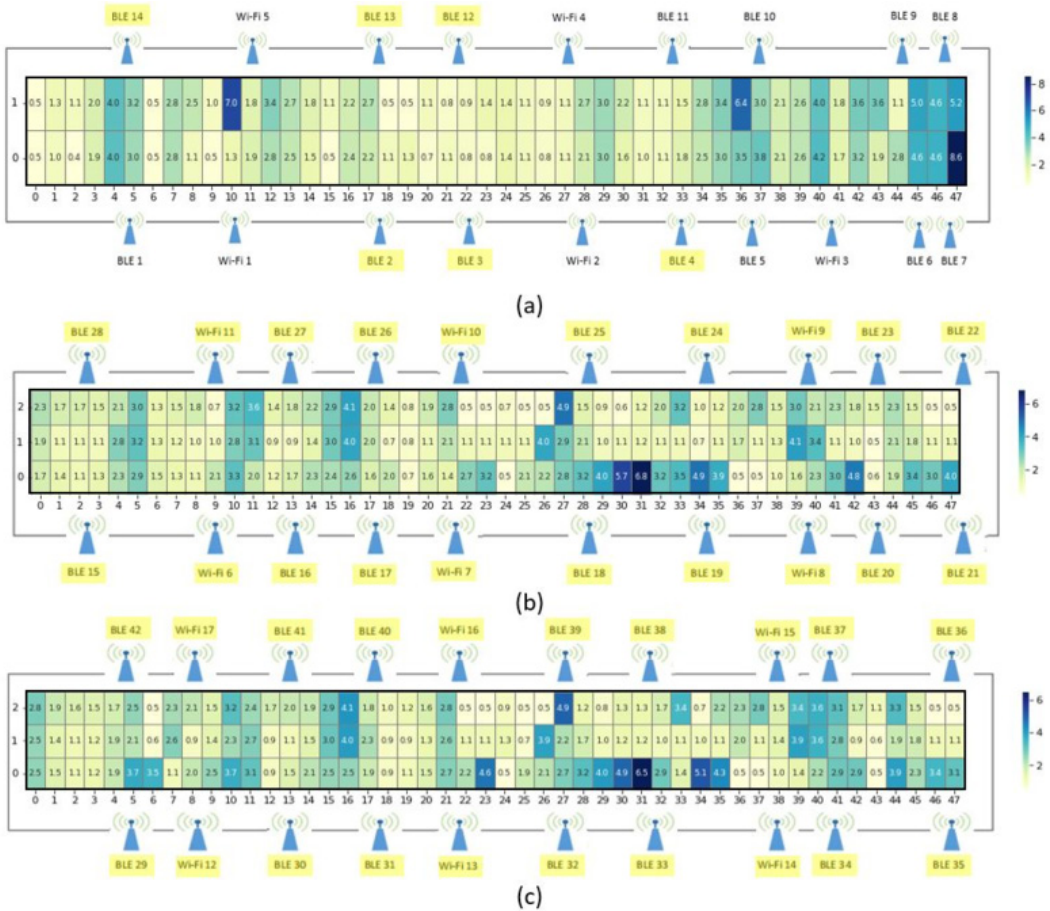
Figure 6. Heatmap of positioning errors for baseline technique in scenario 1: (a) ground floor; (b) first floor; (c) second floor



first, and second floors, and overall, improve 6.58%, 3.67%, 2%, and 3.77%, respectively, whereas, for Scenario 2, the improvements in average positioning errors are 6.28%, 3.81%, 1.87%, and 3.70% for the ground, first, and second floors, and overall, respectively. As expected, the proposed technique yields higher performance gains over the baseline method, particularly on floors with zones that have fewer active APs.

Figure 12 provides an insight into the 95th percentiles of positioning errors for each zone of each floor and overall across all the three floors for both Scenarios 1 and 2. Generally, the 95th percentiles of the proposed optimized RSS-based radio map interpolation technique for most zones are lower than that of the baseline technique. Certain zones of the floors in both scenarios can produce 95th percentiles, up to 13.18% lower than the baseline technique. This observation implies that certain zones indeed require a higher density of known RPs assigned to them for a better indoor location prediction. Moreover, among the 95th percentiles for the individual floors in Scenario 1, the performance recorded on the ground floor results in the 95th percentile of 16.54% lower than the baseline method. In Scenario 2, the ground floor also achieves the 95th percentile of 26.07% lower than the baseline. Overall, for the three floors in Scenario 1, the 95th percentile of the proposed optimized RSS-based radio map interpolation technique is 10.80% lower than that of the baseline technique. Therefore, the

Figure 7. Heatmap of positioning errors for proposed technique in scenario 1: (a) ground floor; (b) first floor; (c) second floor



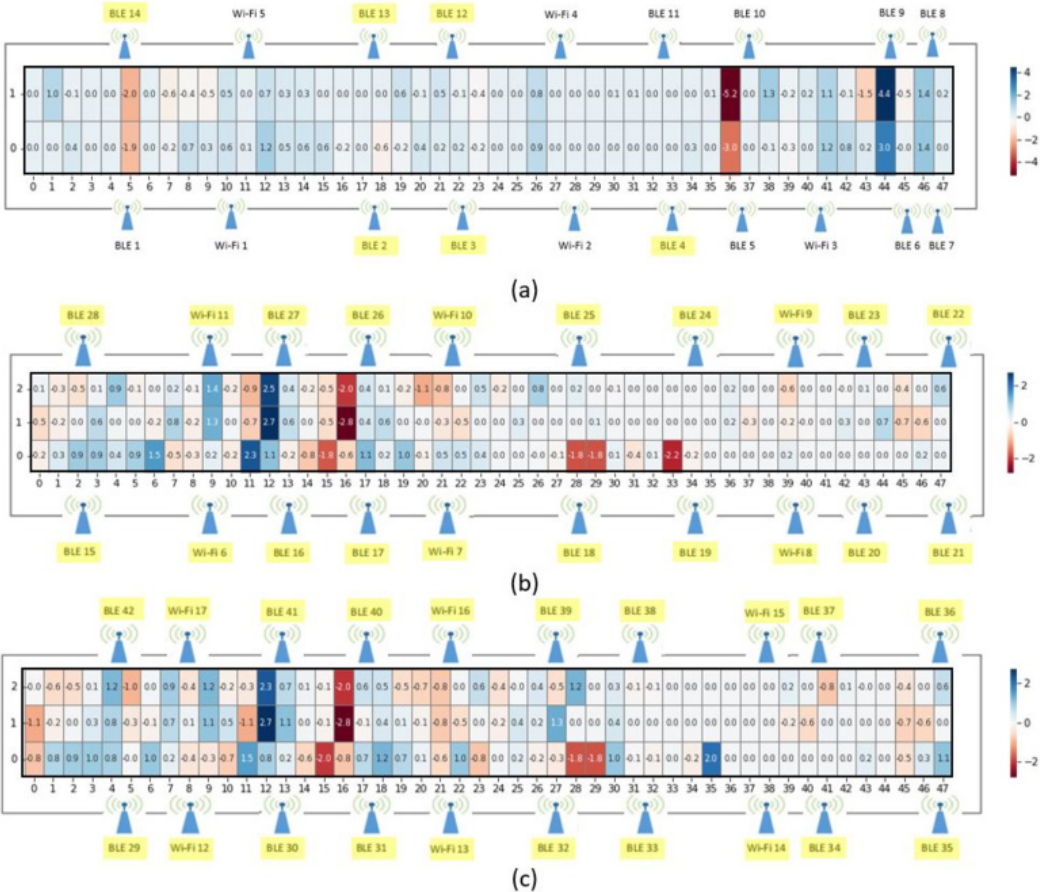
proposed technique that utilizes the RSS strength measured from neighboring APs to determine the appropriate zone-based density of the known RPs is shown to be effective.

CONCLUSIONS

This paper proposes a novel approach for optimizing the zone-based density of the known RPs by considering the number of APs whose average RSS values exceed the threshold RSS to further improve the average positioning error achievable by a uniform zone-based density and distribution of known RPs. In multi-floor indoor environments, zones may be distant from APs on the same floor but located near to APs on the floor directly above or below. Thus, instead of relying only on the distance between the zones and APs to vary the density of the known RPs of the zone, the sufficiency of strong APs can be used as a guideline to determine whether there is a need to increase the density of the known RPs for each zone.

Notably, our results reveal that the proposed optimized RSS-based radio map interpolation approach exhibits significantly superior localization performance compared to the baseline approach utilizing uniform zone-based and known RP distribution. In Scenario 1, the proposed technique achieves remarkable improvements of 6.58%, 3.67%, and 2%, for the ground floor, first floor, and second floor, respectively, resulting in an overall improvement of 3.77% for all three floors. Similarly,

Figure 8. Heatmap of differences in positioning errors between baseline and proposed techniques for scenario 1: (a) ground floor; (b) first floor; (c) second floor



in Scenario 2, the proposed scheme showcases a substantial enhancement of 6.28%, 3.81%, and 1.87%, for the ground floor, first floor, and second floor, respectively, leading to an overall improvement of 3.70% for all three floors. Therefore, the proposed radio map interpolation technique is a practical and highly promising solution for providing accurate large-scale indoor positioning in real-world complex indoor environments. Since the current work primarily focuses on two-dimensional interpolation for multi-floor indoor environments, future research may explore extending the RSS-based interpolation technique to encompass three-dimensional indoor environments. Additionally, integrating it with multiple interpolation methods could further enhance its localization performance by leveraging their respective strengths.

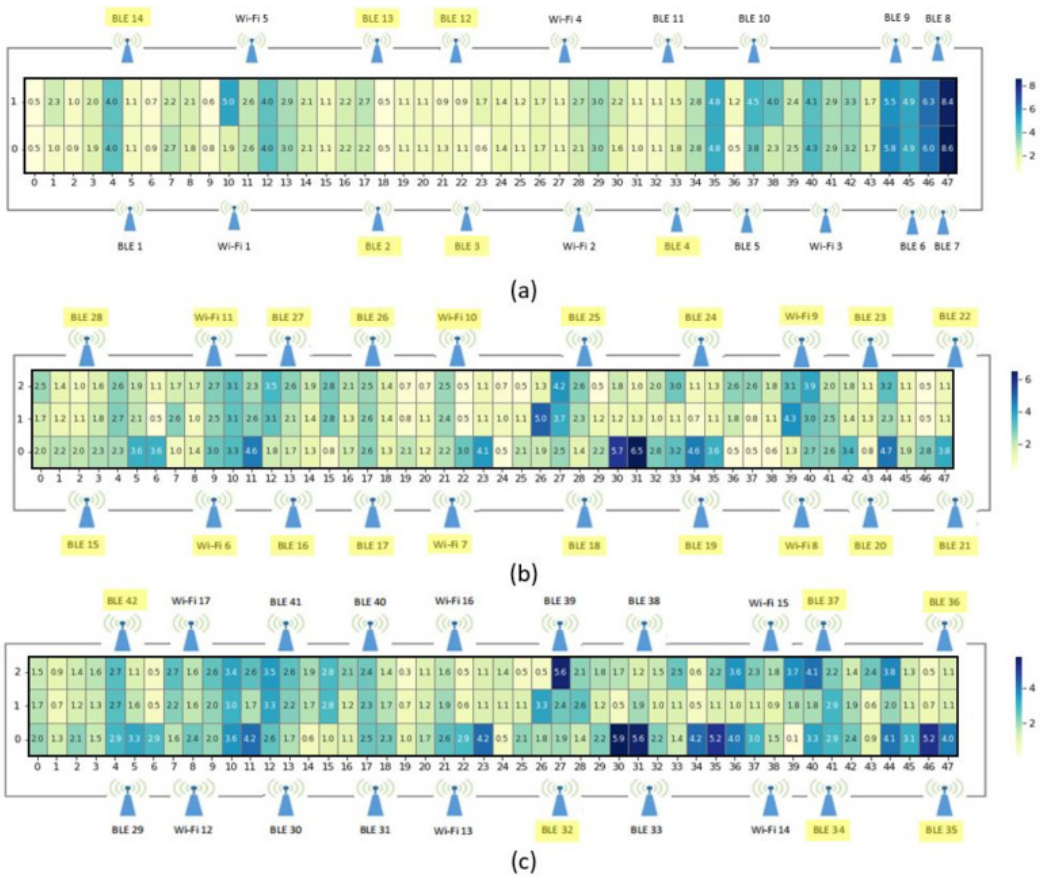
AUTHOR NOTE

Yin Hoe Ng (<https://orcid.org/0000-0002-9854-0384>)

Funding statement: This research was funded by the Ministry of Higher Education, Malaysia, grant number FRGS/1/2023/ICT02/MMU/02/7.

Correspondence concerning this article should be addressed to Yin Hoe Ng, Faculty of Engineering, Multimedia University, Cyberjaya 63100, Malaysia. Email: yhng@mmu.edu.my.

Figure 9. Heatmap of positioning errors for baseline technique in scenario 2: (a) ground floor; (b) first floor; (c) second floor



PROCESS DATES

August 26, 2024

Received: August 25, 2023, Revision: May 20, 2024, Accepted: August 4, 2024

Figure 10. Heatmap of positioning errors for proposed technique in scenario 2: (a) ground floor; (b) first floor; (c) second floor

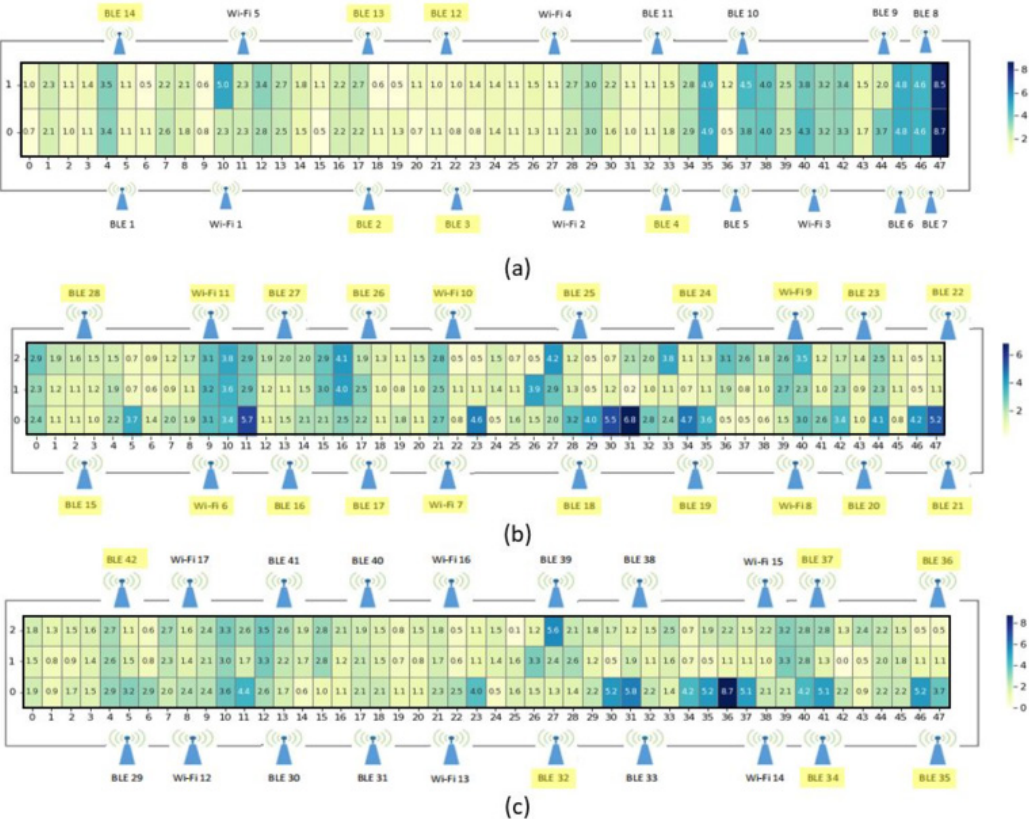


Figure 11. Heatmap of differences in positioning errors between baseline and proposed techniques for scenario 2: (a) ground floor; (b) first floor; (c) second floor

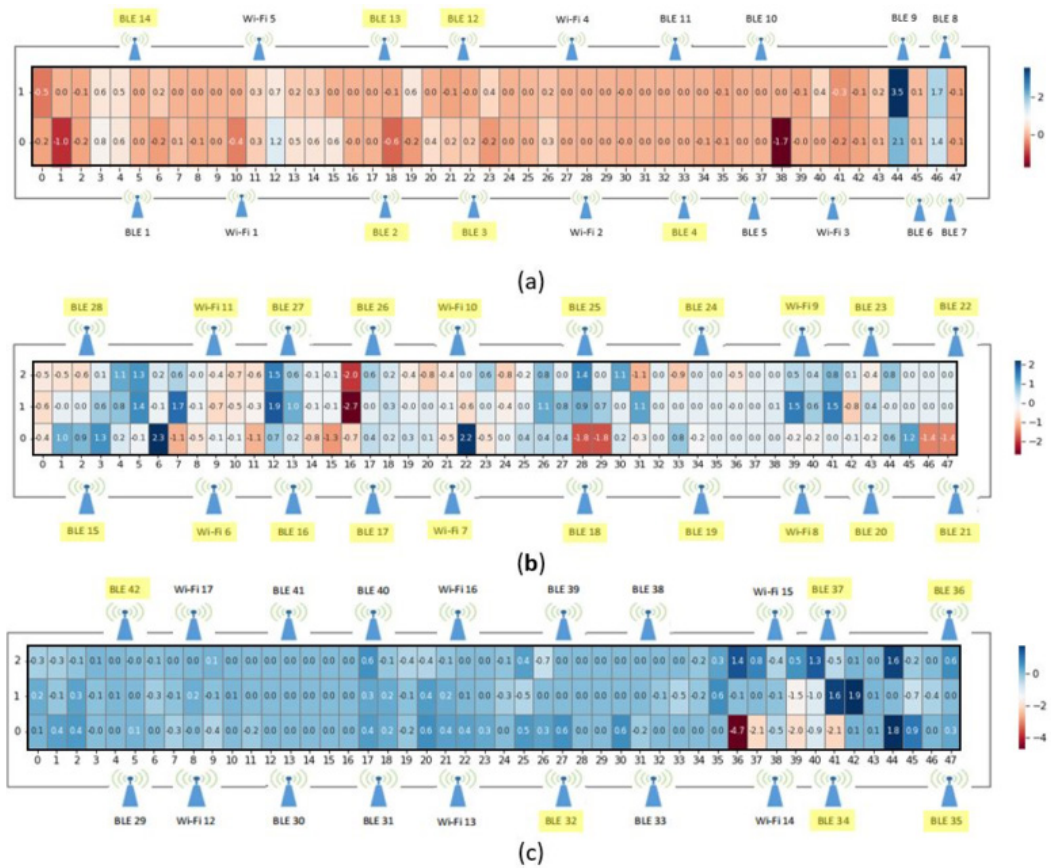
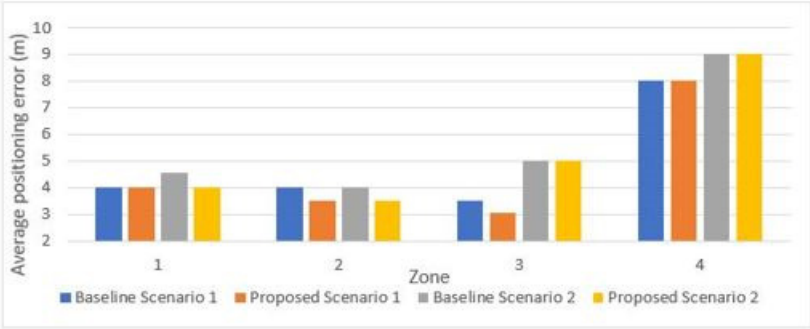
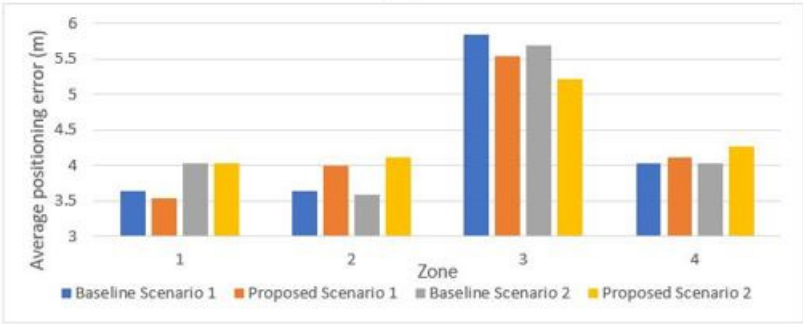


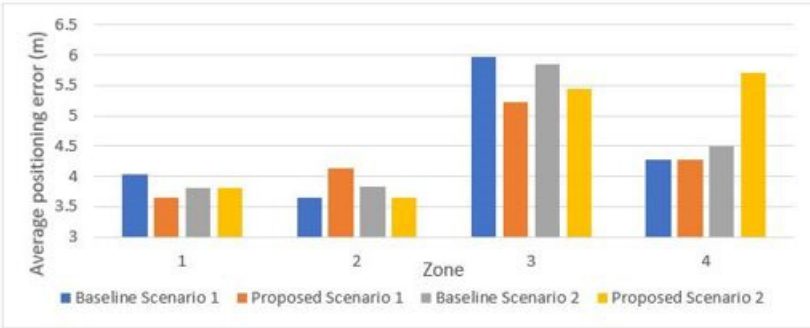
Figure 12. 95th percentiles of positioning errors for: (a) zones of ground floor; (b) zones of first floor; (c) zones of second floor; (d) each individual floor and as an overall



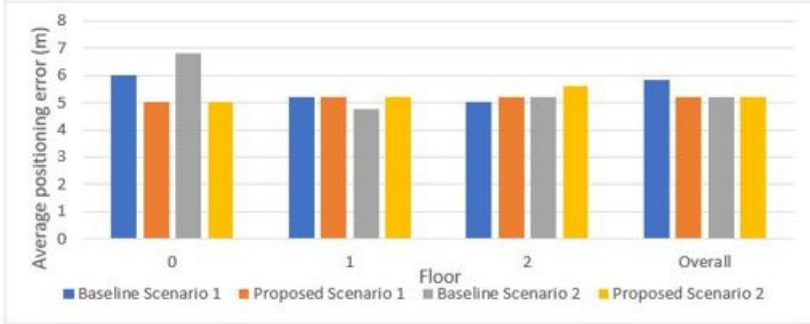
(a)



(b)



(c)



(d)

REFERENCES

- Bi, J., Wang, Y., Cao, H., Qi, H., Liu, K., & Xu, S. (2018). A method of radio map construction based on crowdsourcing and interpolation for Wi-Fi positioning system. In *Proceedings of the 2018 international conference on indoor positioning and indoor navigation (IPIN)* (pp. 1-6). Nantes, France. DOI: 10.1109/IPIN.2018.8533749
- Bi, J., Wang, Y., Li, Z., Xu, S., Zhou, J., Sun, M., & Si, M. (2019). Fast radio map construction by using adaptive path loss model interpolation in large-scale building. *Sensors (Basel)*, 19(3), 1–19. DOI: 10.3390/s19030712 PMID: 30744141
- Boujnah, N., & Korbel, P. (2016). Crowdsourcing based terminal positioning using multidimensional data clustering and interpolation. In *Proceedings of the 2016 federated conference on computer science and information systems* (pp. 961-967). Gdansk, Poland. DOI: 10.15439/2016F337
- Ezhumalai, B., Song, M., & Park, K. (2021). An efficient indoor positioning method based on Wi-Fi RSS fingerprint and classification algorithm. *Sensors (Basel)*, 21(10), 1–19. DOI: 10.3390/s21103418 PMID: 34069023
- Ezpeleta, S., Claver, J. M., Pérez-Solano, J. J., & Marti, J. V. (2015). RF-based location using interpolation functions to reduce fingerprint mapping. *Sensors (Basel)*, 15(10), 27322–27340. DOI: 10.3390/s151027322 PMID: 26516862
- Huang, S., Zhao, K., Zheng, Z., Ji, W., Li, T., & Liao, X. (2021). An optimized fingerprinting-based indoor positioning with Kalman filter and universal kriging for 5G internet of things. *Wireless Communications and Mobile Computing*, 2021(1), 1–10. DOI: 10.1155/2021/9936706
- Huo, Y., Puspitaningayu, P., Funabiki, N., Hamazaki, K., Kuribayashi, M., & Kojima, K. (2021). A parameter optimization method for fingerprint-based indoor localization system using IEEE 802.15.4 devices. In *Proceedings of the 3rd international conference on computer communication and the internet (ICCCI)* (pp. 136-140). Nagoya, Japan. DOI: 10.1109/ICCCI151764.2021.9486801
- Huo, Y., Puspitaningayu, P., Funabiki, N., Hamazaki, K., Kuribayashi, M., & Kojima, K. (2022). A proposal of the fingerprint optimization method for the fingerprint-based indoor localization system with IEEE 802.15.4 devices. *Information (Basel)*, 13(5), 211. DOI: 10.3390/info13050211
- Jan, S. S., Yeh, S. J., & Liu, Y. W. (2015). Received signal strength database interpolation by kriging for a Wi-Fi indoor positioning system. *Sensors (Basel)*, 15(9), 21377–21393. DOI: 10.3390/s150921377 PMID: 26343673
- Ji, T., Li, W., Zhu, X., & Liu, M. (2022). Survey on indoor fingerprint localization for BLE. In *Proceedings of the IEEE 6th information technology and mechatronics engineering conference (ITOEC)* (pp. 129-134). Chongqing, China. DOI: 10.1109/ITOEC53115.2022.9734528
- Khalajmehrabadi, A., Gatsis, N., & Akopian, D. (2017a). Modern WLAN fingerprinting indoor positioning methods and deployment challenges. *IEEE Communications Surveys and Tutorials*, 19(3), 1974–2002. DOI: 10.1109/COMST.2017.2671454
- Khalajmehrabadi, A., Gatsis, N., & Akopian, D. (2017b). Structured group sparsity: A novel indoor WLAN localization, outlier detection, and radio map interpolation scheme. *IEEE Transactions on Vehicular Technology*, 66(7), 6498–6510. DOI: 10.1109/TVT.2016.2631980
- Kiring, A., Yew, H. T., Farm, Y. Y., Chung, S. K., Wong, F., & Chekima, A. (2020). Wi-Fi radio map interpolation with sparse and correlated received signal strength measurements for indoor positioning. In *Proceedings of the 2020 IEEE 2nd international conference on artificial intelligence in engineering and technology (IICAET)* (pp. 1-5). Kota Kinabalu, Malaysia. DOI: 10.1109/IICAET49801.2020.9257857
- Nabati, M., Ghorashi, S. A., & Shahbazian, R. (2020). Joint coordinate optimization in fingerprint-based indoor positioning. *IEEE Communications Letters*, 25(4), 1192–1195. DOI: 10.1109/LCOMM.2020.3047352
- Nor Hisham, A. N., Ng, Y. H., Tan, C. K., & David, C. (2022). Hybrid Wi-Fi and BLE fingerprinting dataset for multi-floor indoor environments with different layouts. *Data*, 7(11), 1–20. DOI: 10.3390/data7110156
- Racko, J., Machaj, J., & Brida, P. (2017). Wi-Fi fingerprint radio map creation by using interpolation. *Procedia Engineering*, 192, 753–758. DOI: 10.1016/j.proeng.2017.06.130

- Redondi, A. E. C. (2018). Radio map interpolation using graph signal processing. *IEEE Communications Letters*, 22(1), 153–156. DOI: 10.1109/LCOMM.2017.2762318
- Shang, S., & Wang, L. (2022). Overview of Wi-Fi fingerprinting-based indoor positioning. *IET Communications*, 16(7), 725–733. DOI: 10.1049/cmu2.12386
- Suto, K., Bannai, S., Sato, K., Inage, K., Adachi, K., & Fujii, T. (2021). Image-driven spatial interpolation with deep learning for radio map construction. *IEEE Wireless Communications Letters*, 10(6), 1222–1226. DOI: 10.1109/LWC.2021.3062666
- Talvitie, J., Renfors, M., & Lohan, E. S. (2015). Distance-based interpolation and extrapolation methods for RSS-based localization with indoor wireless signals. *IEEE Transactions on Vehicular Technology*, 64(4), 1340–1353. DOI: 10.1109/TVT.2015.2397598
- Tan, K. G., Khaing, Z. A., Moe, S. A., Min, T. S., Abdaziz, A., Chia, P. L., Hossain, F., Chih, P. T., & Wong, H. Y. (2021). Review of indoor positioning: Radio wave technology. *Applied Sciences (Basel, Switzerland)*, 11(1), 1–44.
- Tian, X., Li, W., Yang, Y., Zhang, Z., & Wang, X. (2017). Optimization of fingerprints reporting strategy for WLAN indoor localization. *IEEE Transactions on Mobile Computing*, 17(2), 390–403. DOI: 10.1109/TMC.2017.2715820
- Wang, D., Li, L., Hu, C., Li, Q., Chen, X., & Huang, P. (2019). A modified inverse distance weighting method for interpolation in open public places based on Wi-Fi probe data. *Journal of Advanced Transportation*, 2019, 1–11. DOI: 10.1155/2019/7602792
- Wang, J., & Park, J. (2021). An enhanced indoor positioning algorithm based on fingerprint using fine-grained CSI and RSSI measurements of IEEE 802.11n WLAN. *Sensors (Basel)*, 21(8), 1–25. DOI: 10.3390/s21082769 PMID: 33919921
- Wang, Z., Zhang, L., Kong, Q., & Wang, K. (2021). Fast construction of the radio map based on the improved low-rank matrix completion and recovery method for an indoor positioning system. *Journal of Sensors*, 2021(1), 1–12. DOI: 10.1155/2021/2017208
- Ye, Y., & Wang, B. (2018). RMapCS: Radio map construction from crowdsourced samples for indoor localization. *IEEE Access : Practical Innovations, Open Solutions*, 6, 24224–24238. DOI: 10.1109/ACCESS.2018.2830415
- Zhao, H., Huang, B., & Jia, B. (2016). Applying kriging interpolation for Wi-Fi fingerprinting based indoor positioning systems. In *Proceedings of the 2016 IEEE wireless communications and networking conference* (pp. 1-6). Doha, Qatar.
- Zuo, J., Liu, S., Xia, H., & Qiao, Y. (2018). Multi-phase fingerprint map based on interpolation for indoor localization using iBeacons. *IEEE Sensors Journal*, 18(8), 3351–3359. DOI: 10.1109/JSEN.2018.2789431

Hui Wen Khoo was born in Penang, Malaysia, in 1999. She received the BEng degree in electronics engineering (nanotechnology) from Multimedia University in 2022. Her research interests include machine learning and indoor positioning.

Yin Hoe Ng received the BEng degree (Hons.) in electronics engineering, the MEngSc and PhD degrees from Multimedia University in 2004, 2008, and 2013, respectively. He is currently an associate professor in the Faculty of Engineering at Multimedia University. He is also a Chartered Engineer (CEng) and a professional technologist (PTech) registered with the Engineering Council United Kingdom and the Malaysia Board of Technologists, respectively. His current research interests include advanced signal processing techniques for digital communication systems, machine learning, and indoor positioning.

Chee Keong Tan received the BEng degree in electronics (telecommunication), the MEngSc degree in information, communication and technology and the PhD degree in information, communication, and technology from Multimedia University, Malaysia. He is currently a senior lecturer in the School of Information Technology, Monash University Malaysia. He has carried out projects for telecommunication companies and cellular service providers, which led to the development of a few patents on wireless algorithm and protocol design. He is one of the main contributing authors to more than 20 international journal articles. His current research interests include radio resource management, 5G networks, indoor positioning schemes, game theory, machine learning, and artificial intelligence.